Toxicon 164 (2019) 71–81

Contents lists available at ScienceDirect

Toxicon

journal homepage: www.elsevier.com/locate/toxicon

Unveiling toxicological aspects of venom from the Aesculapian False Coral Snake *Erythrolamprus aesculapii*

Matías N. Sánchez[a], Gladys P. Teibler[b], Juliana M. Sciani[c], Milena G. Casafús[a], Silvana L. Maruñak[b], Stephen P. Mackessy[d], María E. Peichoto[a,*]

[a] Consejo Nacional de Investigaciones Científicas y Técnicas (CONICET), Instituto Nacional de Medicina Tropical (INMeT), Neuquén y Jujuy s/n, 3370, Puerto Iguazú, Argentina
[b] Facultad de Ciencias Veterinarias (FCV), Universidad Nacional del Nordeste (UNNE). Sargento Cabral 2139, 3400, Corrientes, Argentina
[c] Laboratório Multidisciplinar de Pesquisa, Universidade São Francisco, Av. São Francisco de Assis, 218, 12916-900, Bragança Paulista, SP, Brazil
[d] School of Biological Sciences, University of Northern Colorado, 501 20th St., CB 92, Greeley, CO, 80639-0017, USA

ARTICLE INFO

Keywords:
Colubrid
Enzymes
Gland histology
Maxilla morphology
Rear-fanged snake
Toxins

ABSTRACT

Most colubrid snake venoms have been poorly studied, despite the fact that they represent a great resource for biological, ecological, toxinological and pharmacological research. Herein, we explore the venom delivery system of the Aesculapian False Coral Snake *Erythrolamprus aesculapii* as well as some biochemical and toxicological properties of its venom. Its Duvernoy's venom gland is composed of serous secretory cells arranged in densely packed secretory tubules, and the most striking feature of its fang is their double-curved shape, exhibiting a beveled bladelike appearance near the tips. Although *E. aesculapii* resembles elapid snakes of the genus *Micrurus* in color pattern, this species produces a venom reminiscent of viperid venoms, containing mainly tissue-damaging toxins such as proteinases. Prominent hemorrhage developed both locally and systemically in mice injected with the venom, and the minimum hemorrhagic dose was found to be 18.8 μg/mouse; the lethal dose, determined in mice, was 9.5 ± 3.7 μg/g body weight. This work has toxicological implications that bites to humans by *E. aesculapii* could result in moderately severe local (and perhaps systemic) hemorrhage and gives insight into future directions for research on the venom of this species.

1. Introduction

Rear-fanged "colubrid" snakes are often considered as non-venomous to humans because most reported accidents available in the literature describe primarily local effects. Additionally, non-aggressive behavior is observed in many species and bites from most species rarely result in complications. Largely because of this perception of harmlessness, rear-fanged snake venoms remain relatively unexplored when compared to the extensive literature concerning the composition and biochemical properties of venoms from front-fanged elapid and viperid snakes. However, during the last few years, there has been a growing interest in the study of rear-fanged venoms, especially those from South America (Junqueira-de-Azevedo et al., 2016), and interesting and sometimes unique biological and enzymatic properties have been demonstrated in these venoms (Modahl et al., 2018b; Saviola et al., 2014).

Erythrolamprus aesculapii is a colorful colubrid snake from South America, commonly known as a false coral snake due to its particular mimicry with medically important *Micrurus* spp. (coral snakes; family Elapidae) (Fig. 1). In Argentina, this species is limited to Misiones province and records of encounters are mainly in the Iguazu National Park (Arzamendia and Giraudo, 2012), an international tourist destination that is visited by more than a million people per year. This tricolored false coral snake displays diurnal habits and its diet consists mainly of snakes (Giraudo, 2014). According to Braz and Marques (2016), a particularly noteworthy trophic feature of this species is the tail-first ingestion of its prey.

Due to its mimicry with true coral snakes and its non-aggressive behavior (Giraudo, 2014), *E. aesculapii* has become a popular pet species, and it has become readily available through the exotic pet trade. Although envenomation by this snake species was reported long ago by Quelch (1893) and mentioned by Lema (1978) and Minton (1990), the public is not generally aware of its potential danger. Herein, we aimed to study the biochemical composition and some biological activities related to the toxicity of the Duvernoy's venom gland secretion (DVGS) of *E. aesculapii* from Argentina, as well as explore its venom delivery system.

* Corresponding author.
E-mail addresses: mepeichoto@yahoo.com.ar, mepeichoto@conicet.gov.ar (M.E. Peichoto).

https://doi.org/10.1016/j.toxicon.2019.04.007
Received 23 February 2019; Received in revised form 8 April 2019; Accepted 12 April 2019
Available online 15 April 2019
0041-0101/

Fig. 1. Specimen of *E. aesculapii* from the Iguazu National Park (Misiones). **A**. Note the diads of black rings that differentiate *E. aesculapii* from Argentinian *Micrurus* snakes (triads or monads of black rings between red bands). Photograph by Ariel López. **B.** Venom extraction procedure; expressed venom can be seen in the capillary tube (bracket). (For interpretation of the references to color in this figure legend, the reader is referred to the Web version of this article.)

2. Materials and methods

Peptide substrate Abz-GPLGWARQ-EDDnp was purchased from Bachem AG (Switzerland). Low-range Rainbow and broad-range molecular mass markers were purchased from GE Healthcare (USA) and Bio-Rad (USA), respectively. The Qubit kit was purchased from Thermo Fisher Scientific (USA). All other biochemicals (reagent grade or better) were purchased from Sigma Chemical Co. (St. Louis, MO, USA).

2.1. Gland histology and histochemistry

Freshly dead specimens of *E. aesculapii,* obtained from the serpentariums of the Centro Interactivo de Serpientes Venenosas de Argentina (CISVA, Argentina) and the National Institute of Tropical Medicine (INMeT, Argentina) were used to analyze the histological characteristics of its DVG. Glands were removed, fixed in phosphate-buffered 10% formaldehyde (pH 7.2), and embedded in paraffin for classical histological techniques. Then, 5 µm sections were stained with hematoxylin-eosin (H&E) for general histology. For histochemical evaluation, periodic acid-Schiff (PAS) and Alcian Blue (AB, pH 2.5) staining was performed.

2.2. Structure of maxillae and fangs

Maxillae and the maxillary teeth were studied by scanning electron microscopy (SEM). In order to prepare the samples, soft tissues were removed manually, maxillae cleaned and then mounted on a stub with double-sided tape. Samples were then critical-point dried, coated with a thin layer of gold (Denton Vacuum Desk II) and examined using a JEOL 5800LV scanning electron microscope at an acceleration voltage of 15 kV.

2.3. Biochemical and toxicological analysis of E. aesculapii venom

2.3.1. Venom extraction

Extractions were carried out as described by Sanchez et al. (2018) and shown in Fig. 1. Due to restricted distribution, habitat loss (mainly due to deforestation of the Interior Atlantic Forest), human persecution because of its appearance similar to coral snakes, and its low reproductive potential, *E. aesculapii* is considered as a snake species threatened with extinction in Argentina (Arzamendia and Giraudo, 2012). For this reason, venom (including samples from several extractions) from only one specimen of *E. aesculapii* (an adult female) captured in the Iguazu National Park (Misiones, Argentina) - in accordance with authorization from the National Park Administration (APN N° 335/13) - was used for this study. When required, the venom was freshly dissolved in phosphate buffered saline (PBS) pH 7.4 and the protein content was determined by fluorometry using a Qubit 2.0 (Life Technologies, USA).

2.3.2. Gel electrophoresis

The protein profile of *E. aesculapii* venom was analyzed by sodium dodecyl sulfate–polyacrylamide gel electrophoresis (SDS-PAGE) using 4% stacking and 12% resolving gels (Laemmli, 1970), and Tricine SDS-PAGE using 4% stacking, 10% spacer and 16.5% resolving gels (Schägger and von Jagow, 1987). In both cases, samples were run under reducing (with 2-mercaptoethanol) and non-reducing (without 2-mercaptoethanol) conditions. Each lane was loaded with 2.5 µg of protein, and gels were then silver stained (Blum et al., 1987).

2.3.3. Mass spectrometry

Venom of *E. aesculapii* was also analyzed using a Bruker Microflex LRF MALDI-TOF mass spectrometer at the Proteomics and Metabolomics Facility at Colorado State University (Fort Collins, CO). Briefly, 1.0 µg protein dissolved in 1.0 µL 50% acetonitrile containing 0.1% TFA was mixed with 1.0 µL sinapinic acid matrix (10 mg/mL, dissolved in the same solvent), and then spotted onto target plates, dried and followed by a brief isopropanol wash (2.5 µL) to remove salts. Operating in linear mode, spectra were acquired in the mass range of 2.0–40 kDa and tentatively identified based on mass similarity with known colubrid toxins (Pla et al., 2018).

For identification of the main components in the venom, protein target bands were excised from 12% SDS-PAGE and Tricine-SDS-PAGE gels stained with Coomassie Brilliant Blue G 250. Protein digestion and mass spectrometry analysis were performed at the Proteomics Core Facility, CEQUIBIEM, at the University of Buenos Aires/CONICET as follows: excised protein bands were sequentially washed with 50 µL of 50 mM ammonium bicarbonate (AB), 25 mM AB, 50% ACN, and 100% ACN; reduced and alkylated with 10 mM dithiothreitol (DTT) and 55 mM iodoacetamide (IAA), and in-gel digested with 100 ng Trypsin (Promega V5111) in 25 mM AB overnight at 37 °C. Peptides were recovered by elution with 50% ACN/0.5% TFA, including brief sonication, and then further concentrated by speed-vacuum drying. Samples were resuspended in 15 µL of water containing 0.1% formic acid (FA), desalted using C18 zip tips (Merck Millipore), and eluted in 10 µL of H_2O:ACN:FA 40:60:0.1%. Samples were dried and resuspended in 15 µL of water containing 0.1% FA. Digests were analyzed by nanoLC-MS/MS in a nanoHPLC EASY-nLC 1000 (Thermo Scientific) coupled to a QExactive Mass Spectrometer. A 75-min gradient of H_2O:ACN at a flow of 33 nL/min was used with a C18 2 mm × 150 mm Easy Spray column. Data-dependent MS2 method was used to fragment the top 15 peaks in each cycle. The raw data from mass spectrometry analysis were processed using the Proteome Discoverer, version 2.1.1.21 (Thermo Scientific) software for database searching with the SEQUEST search algorithm. The search was performed against a Uniprot database (https://www.uniprot.org/uniprot/?query=venom+snake&sort=score) generated using 'snake' and 'venom' as keywords. In the search parameters trypsin was selected as the enzyme used. Precursor mass tolerance was set to 10 ppm and product ion tolerance to 0.05 Da. Static modification was set to carbamidomethylation of Cys, and dynamic

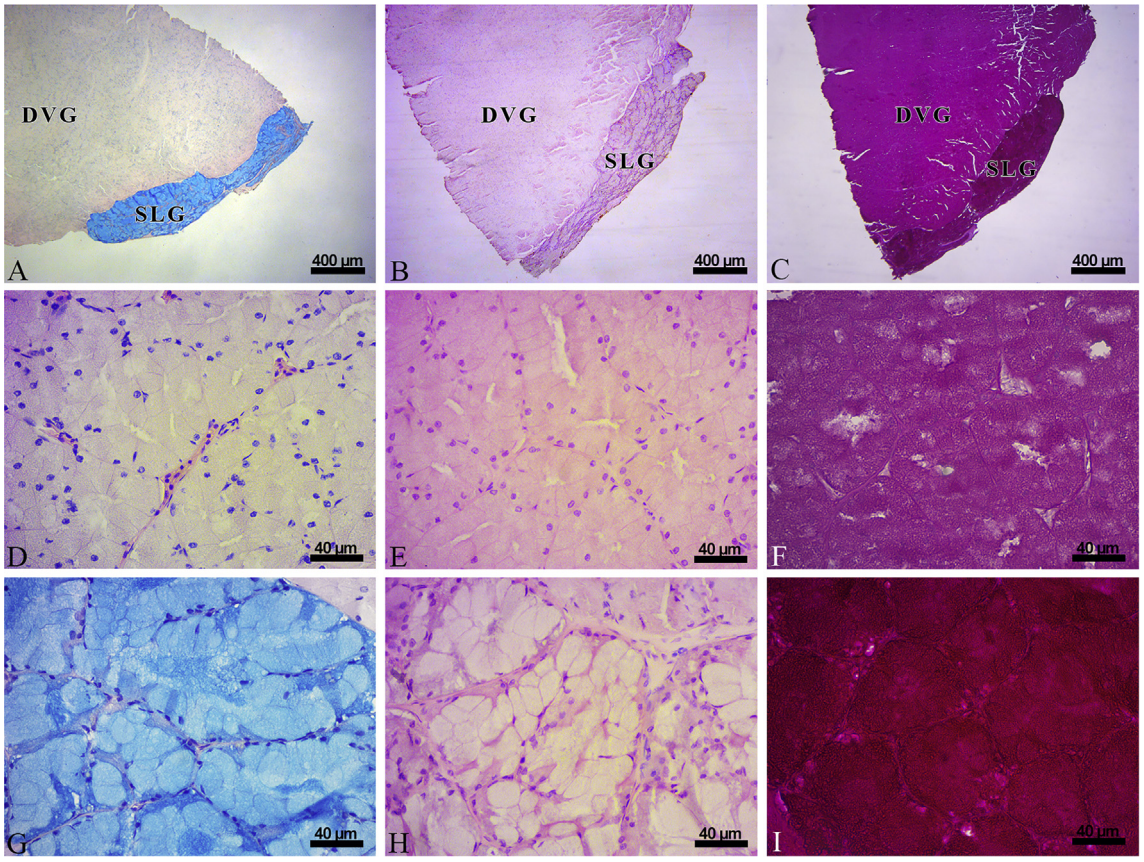

Fig. 2. Histology and histochemistry of the supralabial (SLG) and Duvernoy's venom (DVG) glands of *E. aesculapii*. **A, B and C**. Cross-section of both glands with alcian blue (pH 2.5) (AB), hematoxylin/eosin (H&E) and periodic acid-Schiffs (PAS) staining, respectively. Note the differential color intensity associated with the different nature of the glands (serous: DVG; mucous: SLG). **D, E and F**. Cross-section of DVG with AB, H&E and PAS staining, respectively. Note secretory tubules lined with serous columnar cells with basal round nuclei. **G, H and I**. Cross-section of SLG with AB, H&E and PAS staining, respectively. Note lobes defined by connective tissue septa and globular cells filled with acid mucopolysaccharides. (For interpretation of the references to color in this figure legend, the reader is referred to the Web version of this article.)

modifications were set to oxidation of Met and N-terminal acetylation. Protein hits were filtered for high confidence peptide matches with a maximum protein and peptide false discovery rate of 1% calculated by employing a reverse database strategy.

2.3.4. Quantitative enzyme assays

Enzymatic activity toward collagen and hyaluronic acid, two of the main components of connective tissue, were determined as reported previously (Sanchez et al., 2018). One unit of collagenolytic activity was defined as the amount of venom protein that causes an increase of 0.003 units of absorbance per min at 540 nm and the specific activity was expressed as U/mg protein. For hyaluronidase activity, the value was expressed as degraded hyaluronic acid/min/mg protein. In addition, proteolytic activity toward azocasein was measured by a previously reported method (Quintana et al., 2017). The amount of protein that causes an increase of 0.005 units of absorbance per min at 450 nm was defined as one unit of enzymatic activity and the specific activity was expressed as U/mg protein.

The serine proteinase and metalloproteinase activities were measured by the hydrolysis of the synthetic substrates Nα-Benzoyl-L-arginine 4-nitroanilide hydrochloride (L-BAPNA) and Abz-GPLGWARQ-EDDnp, respectively, in a concentration range from 0 to 20 µM. The reactions were conducted in 20 mM Tris-HCl buffer pH 8.5 in a 96-well microplate (in a final volume of 100 µL). For both assays, 10 µg/mL of venom was used. The hydrolysis of L-BAPNA was monitored by spectrophotometer (Epoch Microplate Spectrophotometer, BioTek, USA) at λ = 410 nm for 30 min. The hydrolysis of Abz-GPLGWARQ-EDDnp was monitored by the increase of fluorescence emission (λex = 360 nm and λem = 420 nm) in a GloMax®-Multi Detection System fluorimeter (Promega, USA) for 20 min.

Acetylcholinesterase (AChE) and phospholipase A_2 (PLA_2) activities were assayed according to the methods of Ellman et al. (1961) and Antunes et al. (2010), respectively. All enzyme assays were performed in triplicate. Negative controls were also performed in triplicate.

2.3.5. Fibrin(ogen)olytic activity

Specific cleavage of fibrinogen by *E. aesculapii* venom was determined by SDS-PAGE using 12% polyacrylamide gels as described elsewhere (Sanchez et al., 2018), and under two different conditions, with and without $CaCl_2$ (0.5 mM, final concentration). One hundred and 50 µL of 2 mg/mL human fibrinogen dissolved in 50 mM Tris-HCl buffer (pH 7.4) was incubated with venom (50:1 mass ratio) at 37 °C. At various time intervals, aliquots of 15 µL were withdrawn from the digestion mixture, and then denatured and reduced by boiling for 10 min with 15 µL of denaturing solution (4% SDS, 20% glycerol and 20% 2-mercaptoethanol) prior to gel electrophoresis. For fibrinolytic activity, fibrinogen aliquots (20 µL) were coagulated by adding bovine thrombin (5 U/mL final concentration, Sigma) prior to the addition of venom (50:1 ratio). At different time intervals, 20 µL of denaturing solution were added to the reaction mixture and then processed as above.

2.3.6. Toxicity assays

Venom of *E. aesculapii* was evaluated for lethality, myotoxicity and quantitative determination of hemorrhagic activity using male CF-1 mice weighing 18–20 g. The animals were supplied by the Animal

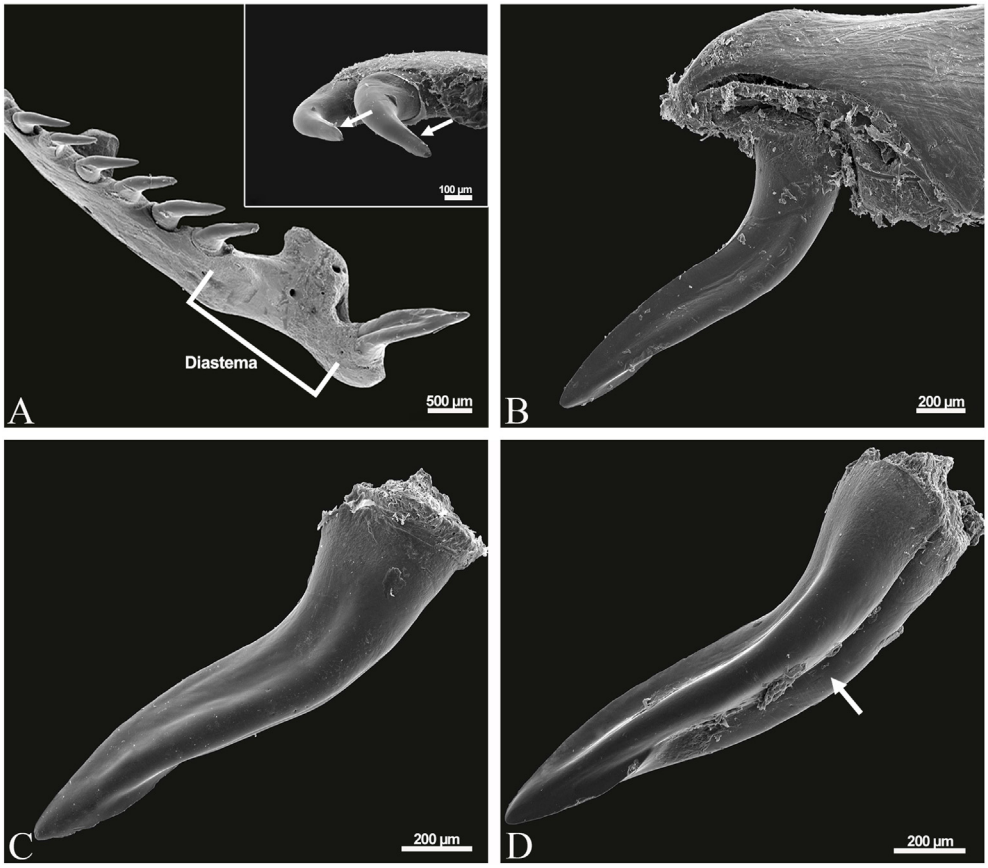

Fig. 3. SEM micrographs of the maxilla and fangs of *E. aesculapii*. **A**. Ventral view showing maxillary teeth separated from the grooved rear fang by a wide diastema. Inset detail: view of anterior teeth with lateral ridges (arrow). **B**. Lingual view showing the back side of the rear fang. **C**. Lateral view showing the double recurved fang, with double sharp ridges (posterior ridge extending from its base to its tip, and anterior ridge extending from its mid-point to its tip), resembling a double-edged knife. **D**. Micrograph showing the deep groove (arrow) along the rostral side.

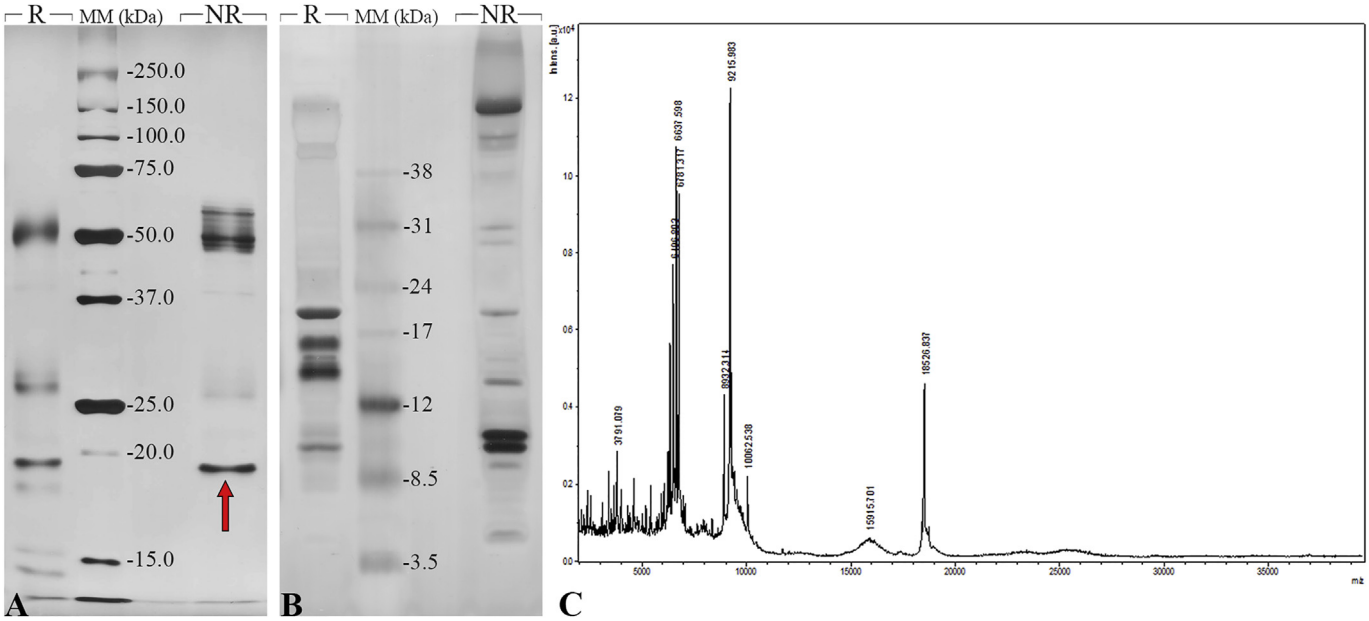

Fig. 4. Electrophoretic profiles and mass spectrogram of *E. aesculapii* venom. **A**. 12% SDS-PAGE. Note the red arrow indicating a ~18 kDa protein band which may correspond to a phospholipase B revealed by MS/MS analysis. **B**. 16.5% Tricine-SDS-PAGE. **C**. MALDI-TOF spectrogram of venom. Gels were silver-stained. R: reducing conditions. NR: non-reducing conditions. MM: molecular mass markers. (For interpretation of the references to color in this figure legend, the reader is referred to the Web version of this article.)

House of the School of Medicine of the University of Northeastern Argentina (UNNE). All the experimental procedures were performed in accordance with the Guide for the Care and Use of Laboratory Animals (National Research Council, 1996) and approved by the Ethical Committee for the Use of Animals of College of Veterinarian Sciences (UNNE) according to protocol Nº 070/17.

2.3.6.1. Lethal toxicity. Briefly, groups of three animals were inoculated intraperitoneally with doses from 0 to 20 µg/g body weight in 100 µL of total volume and monitored periodically for 24 h

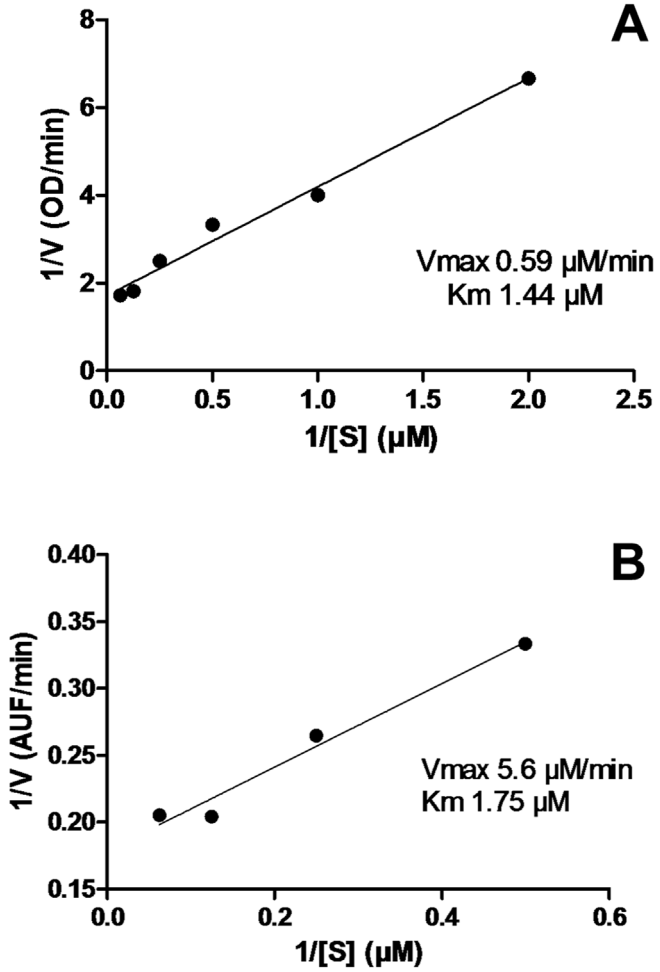

Fig. 5. Double reciprocal plots of reaction velocity as a function of substrate concentration. **A**. Serine proteinase activity toward L-BAPNA. **B**. Metalloproteinase activity toward Abz-GPLGWARQ-EDDnp. Both assays utilized *E. aesculapii* venom at 10 µg/mL reaction mixture.

after injection (Weldon and Mackessy, 2010). Necropsies were performed on animals that succumbed to the venom to analyze further the extent of tissue damage.

2.3.6.2. Myotoxicity. Animals were injected in the right gastrocnemius muscle with 40 µg protein dissolved in 100 µL of PBS (pH 7.4). Control mice were injected with only vehicle under identical conditions. After 1, 3, 6, 9, 12 and 24 h of injection, animals were sacrificed and muscles were dissected. For histological analysis, small samples of muscle were collected and fixed in phosphate-buffered 10% formalin (pH 7.2) for 24–48 h. Thereafter, the samples were dehydrated in an ethanol ascending series, cleared in xylol, and embedded in liquid paraffin. Sections of 5 µm thickness were cut and stained with H&E and examined with a Zeiss Primo Star microscope equipped with a digital camera AxioCam ERc 5s.

2.3.6.3. Hemorrhagic activity. This activity was evaluated as previously described by Sánchez et al. (2014). Different doses of venom (15–125 µg/animal) were injected intradermally in mice, using three animals per dose. Two hours after injection, animals were euthanized, and the skin was removed using a 4 cm diameter punch. Half of the skin removed was immediately cut, fragmented, and added to tubes containing 4 mL of Drabkin's reagent. The tissue fragments were immediately homogenized, and the reaction mixtures were incubated in the absence of light at room temperature for 24 h. Thereafter, tubes were centrifuged at 5000 g for 5 min. The absorbance of the supernatant at 540 nm was determined and then hemoglobin concentration was calculated (Goncalves and Mariano, 2000). The Minimum Hemorrhagic Dose (MHD) was defined as the minimal concentration of venom able to induce a three-fold increase in hemoglobin concentration relative to that of a control tissue injected only with vehicle. The other half of the skin removed was used for histopathology analysis as described above.

2.3.7. Cross-reactivity with elapid and viperid antivenoms used in Argentina

In order to evaluate for the presence of components cross-reacting with anti-*Bothrops* and anti-*Micrurus* horse sera, Western blot analyses were performed. Proteins separated by SDS-PAGE were transferred to 0.2 µm nitrocellulose membranes in a tank transfer system (Hoeffer mini VE, Amersham Biosciences) at 25 V for 1.5 h. Membranes were then blocked with 5% nonfat dry milk, and incubated with tetravalent anti-*Bothrops* or anti-*Micrurus* serum (kindly donated by the Instituto Nacional de Producción de Biológicos from Argentina) diluted 1:500 with 5% nonfat dry milk in PBS (0.1% Tween 20), and subsequently with 1:10,000 peroxidase-conjugated anti-horse IgG (Sigma A9292). The reaction was developed with 3,3′-diaminobenzidine tetrahydrochloride hydrate (DAB, Sigma D5637) as reported elsewhere (Antunes et al., 2010).

2.4. Statistical analyses

Where appropriate, values were expressed as the mean ± standard

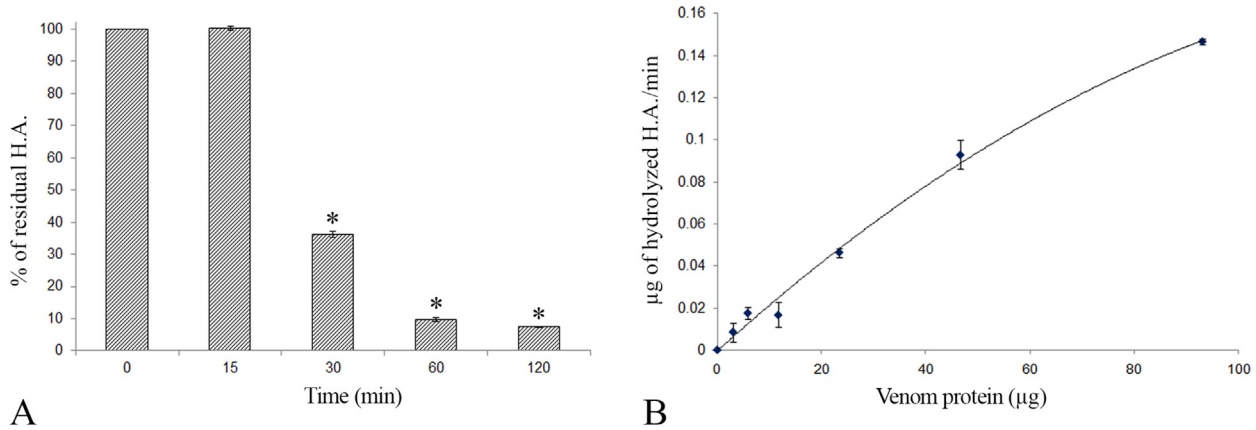

Fig. 6. Hyaluronidase activity of *E. aesculapii* venom. **A**. Time-dependent effect after incubation with 90 µg of venom. **B**. Concentration-dependent effect (120 min incubation). Bars represent the mean ± SD of three individual experiments. *, $p < 0.05$; indicates statistically significant differences with the control (first bar in A). H.A., hyaluronic acid.

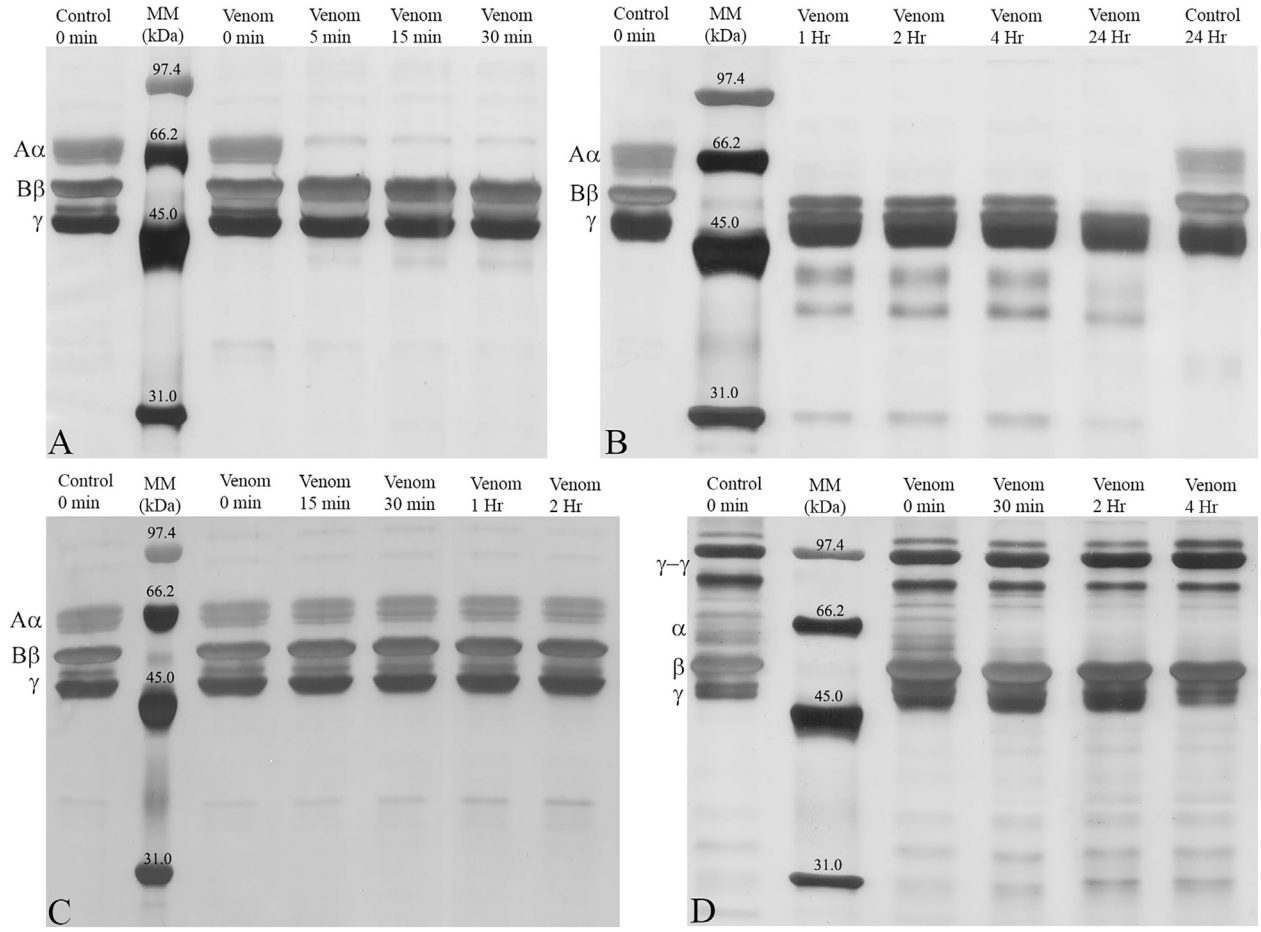

Fig. 7. Time course of the effect of *E. aesculapii* venom on human fibrinogen and fibrin, with and without calcium. In the presence of calcium, degradation of fibrinogen Aα (A) and Bβ (B) chains is observed. Fibrinogen degradation is not observed in the absence of calcium (C). Activity toward fibrin is also observed only in the presence of calcium (D). The assays were evaluated by SDS-PAGE (12%) under reducing conditions. Human fibrinogen chains are indicated (Aα - 63 kDa, Bβ - 56 kDa, and γ - 47 kDa), and the chains of human fibrin are labeled (γ-γ dimer, α-monomer, β-monomer, and γ-monomer). Controls were incubated in absence of the venom, and all gels were silver stained. MM: molecular mass markers.

deviation (SD) and statistical comparisons were done using one-way analysis of variance (ANOVA) followed by Dunnett's test. All data analyses were performed using Infostat Software, with a value of $p < 0.05$ indicating statistical significance.

3. Results

3.1. Histology and histochemistry of supralabial (SLG) and Duvernoy's venom (DVG) glands

Histologically, the DVG of *E. aesculapii* is found separate from the SLG, exhibiting different structural and chemical natures (Fig. 2). The DVG is formed by lobes that are constituted by tubules. Each tubule has a narrow lumen lined by columnar secretory cells that produce venom secreted to the base of the rear fang. Cells from the secretory tubules reacted negatively to PAS and AB staining, indicating the serous nature of this gland. In contrast, the mucous nature of the SLG was demonstrated by the positive reaction to both histochemical stains.

3.2. Morphology of maxillae and fangs

By SEM analysis (N = 3), it was possible to observe that maxilla of *E. aesculapii* possesses 7 to 9 teeth, with a single rear fang that is clearly differentiated from the other teeth by its larger size (Fig. 3). The fang exhibits an atypical double-curved shape, with both anterior and posterior sharpened edges resembling a double-edge knife. Additionally, a deep groove extends along the entire fang.

3.3. Protein profile

Venom yields from *E. aesculapii* averaged 200 µL (50–450 µL, n = 10). By 12% SDS-PAGE and Tricine-SDS-PAGE, the venom of *E. aesculapii* showed a broad distribution of molecules with molecular masses ranging from ~10.0 to 60.0 kDa (Fig. 4A and B); bands at approx. 53 kDa are likely metalloproteinases, common in rear-fanged snake venoms (Mackessy, 2010). MALDI-TOF mass spectrometry mainly revealed peptide/protein components of low molecular masses (Fig. 4C), and masses in the 6–7 and 8–9 kDa ranges are consistent with three-finger toxins (3FTx) from rear-fanged snake venoms. The protein with a mass of 18,527 Da may correspond to a phospholipase B, since the MS/MS-derived sequence of a tryptic peptide from the 18 kDa protein band (indicated by an arrow in Fig. 4A) was matched by SEQUEST to an internal sequence, YSDQTDILR, from a phospholipase B of *Phalotris mertensi* (Uniprot accession N° A0A182C6E9). No other proteins could be identified with a significant score by mass spectrometry.

3.4. Enzyme assays

Venom of *E. aesculapii* exhibited high proteolytic activity, with specific azocollagenolytic and azocaseinolytic activities of 229.9 and 41.5 U/mg respectively. The proteolytic activity of serine and metalloproteinases was detected by the hydrolysis of synthetic substrates.

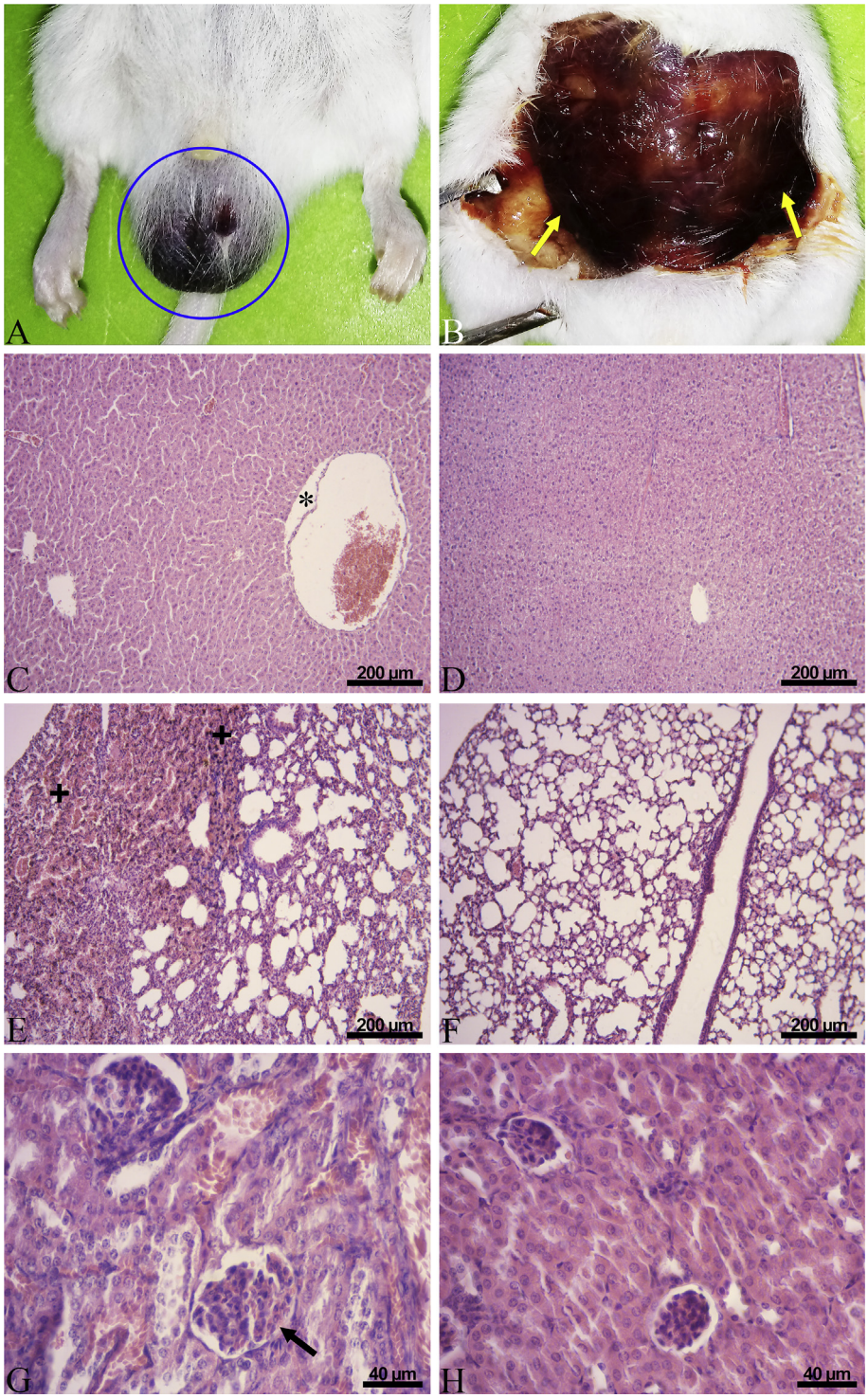

Fig. 8. Systemic effects in mice after intraperitoneal injection of lethal doses (180 μg/animal) of *E. aesculapii* venom. **A**. The scrotal skin (blue circle) shows signs of severe hemorrhage, and a drop of blood is visible. **B**. Intense hemorrhage (yellow arrows) inside the peritoneal cavity. **C**. Histopathological changes induced in liver. Note sinusoidal dilation and detachment of the central vein endothelium (*). **D.** Liver control. **E**. Lung with multiple hemorrhagic foci and hemosiderin deposits (+). Note the thickening of alveolar septa by infiltration of inflammatory leukocytes. **F**. Lung control. **G**. Kidney showing intense glomerular congestion (arrow) with hemorrhage surrounding the glomeruli. **H**. Kidney control. (For interpretation of the references to color in this figure legend, the reader is referred to the Web version of this article.)

Kinetic parameters of Vmax and Km were calculated as 0.59 μM/min and 1.44 μM, respectively, for serine proteinase activity, and 5.60 μM/min and 1.75 μM for metalloproteinase activity of venom (Fig. 5).

Hyaluronidase activity was dependent on both the time of incubation and the amount of venom (Fig. 6); hydrolysis of hyaluronic acid showed a lag time, with rapid hydrolysis occurring after 30 min of incubation (Fig. 6A). In the presence of calcium, the fibrinogen digestion revealed a rapid hydrolysis of the Aα-chain of fibrinogen by 5 min (Fig. 7A), and after 60 min there appeared to be some degradation of the Bβ-chain (Fig. 7B). In the absence of calcium, the venom did not affect fibrinogen (Fig. 7C). For the fibrin digestion assay, the α-monomer was mainly affected (Fig. 7D), but only in the presence of calcium. Neither AChE nor PLA_2 activities were detectable.

3.5. Lethal toxicity

When venom of *E. aesculapii* (> 5 μg/g body weight) was injected intraperitoneally in mice, animals showed abnormal behavior, characterized mainly by apathy and lethargy. The calculated medial lethal dose (LD_{50}) was 9.5 ± 3.7 μg/g body weight. Necropsies for animals that received lethal doses revealed substantial hemorrhage, both locally and systemically, the latter event occurring primarily in the lungs

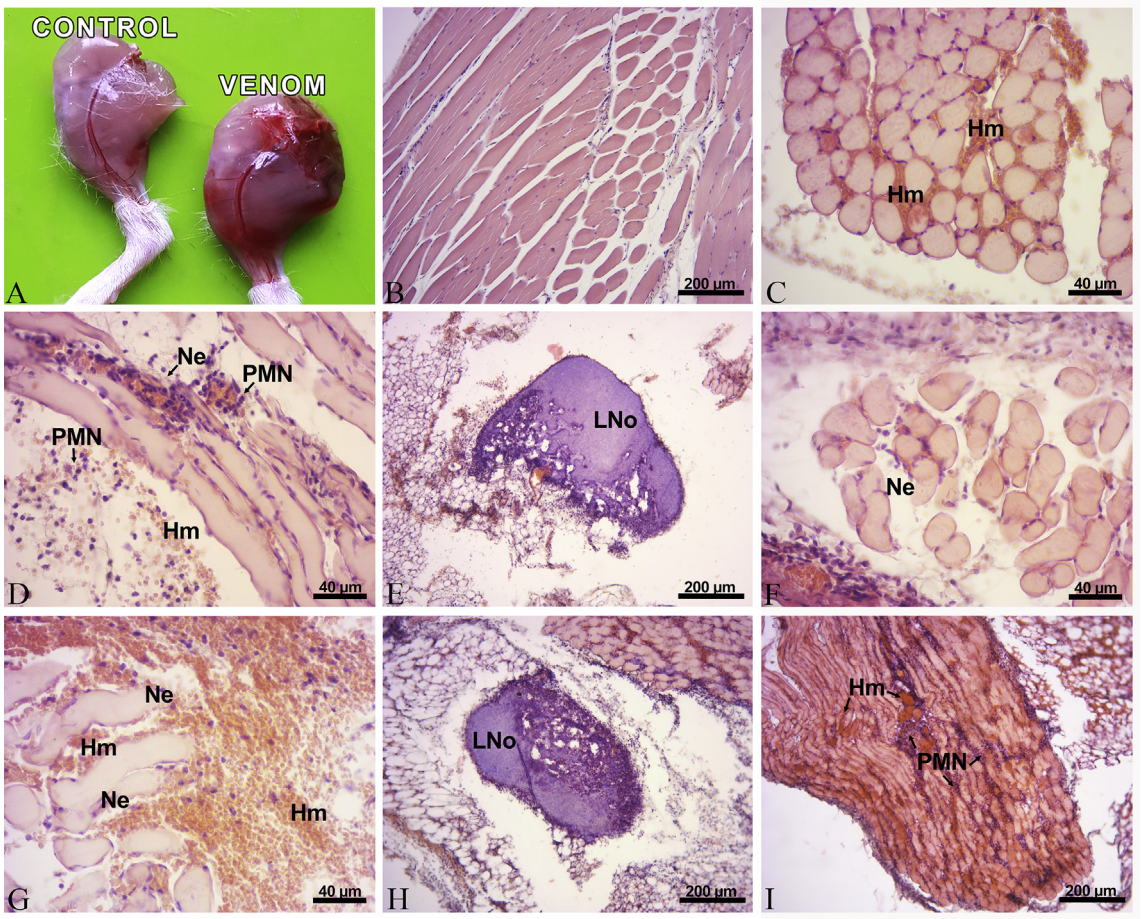

Fig. 9. Light micrographs showing the histopathological changes in mouse gastrocnemius muscle after injection of 40 µg of *E. aesculapii* venom per animal (H&E stain). **A**. Muscles 1 h after injection with PBS (control) or 40 µg of protein (venom). **B**. Longitudinal section of muscle fibers in control group. **C**. Cross-section of muscle 1 h after venom injection; note intense interfibrillar hemorrhage surrounding muscle fibers. **D**. Longitudinal section 1 h after venom injection showing intense neutrophilic inflammatory infiltrate and slight myonecrosis. **E**. Cross-section 3 h after venom injection; note partial destruction of a lymph node. **F**. Cross-section 6 h after venom injection showing necrosis of muscle fibers. **G**. Longitudinal section 9 h after venom injection; extensive hemorrhage and necrosis of muscle fibers are apparent. **H**. Cross-section 12 h after venom injection: note lymph node with destruction of the capsule. **I**. Longitudinal section 24 h after venom injection; hemorrhage is still persisting. **Hm**: hemorrhage; **Ne**: myonecrosis; **PMN**: polymorphonuclear infiltrate; **LNo**: lymph node.

(Fig. 8). Histopathological analysis of the lungs showed multiple hemorrhagic foci with hemosiderin staining and thickening of the alveolar septa due to inflammatory infiltration. In kidneys, intense glomerular congestion and focuses of medullary hemorrhage with hemosiderin deposits were observed. Regarding the liver histological findings, sinusoidal dilatation and congestion as well as centrilobular and periportal necrosis with detachment of the vascular endothelium were revealed.

3.6. Myotoxicity

The macroscopic appearance of the muscle injected with *E. aesculapii* venom was quite different from the control (Fig. 9), characterized by macroscopic hemorrhage observed in venom-treated animals. Conversely, the histopathological analysis revealed only mild myonecrotic activity, but with intense interfibrillar hemorrhage, edema and inflammatory reaction. Complete destruction of the capsule of a nearby lymph node was also observed (Fig. 9).

3.7. Hemorrhagic activity

The venom of *E. aesculapii* induced hemorrhage in a dose-dependent manner after intradermal injection in mice (Fig. 10). The MHD for this venom was 18.8 µg/mouse (1 µg/g body weight). Microscopic analysis by histopathology showed an intense subcutaneous hemorrhage, edema and inflammatory reaction predominantly by neutrophilic leukocytes. When skins of mice inoculated with 60 µg of venom per animal were observed, the hemorrhage and the inflammatory infiltrate were so intense that they extended to the dermis and resulted in the detachment of the epidermis (Fig. 10).

3.8. Cross-reaction with elapid and viperid antivenoms used in Argentina

By Western blotting, several components of the venom of *E. aesculapii* were partially recognized by both tetravalent anti-*Bothrops* and anti-*Micrurus* serum (Fig. 11). Proteins of 50–60 kDa were mostly recognized in both Western blots, but slight bands between 37 and 50 kDa were also detected with the *Micrurus* antivenom.

4. Discussion

Snakes are the major group of vertebrates that produce venoms, and the rear-fanged snakes represent the vast majority of species around the world; however, relatively few studies have characterized their venoms and evaluated their potential hazards for humans (Junqueira-de-Azevedo et al., 2016). Herein, we provide information about the venom delivery system of the Aesculapian False Coral Snake, *Erythrolamprus aesculapii*, as well as a biochemical and toxicological analysis of its

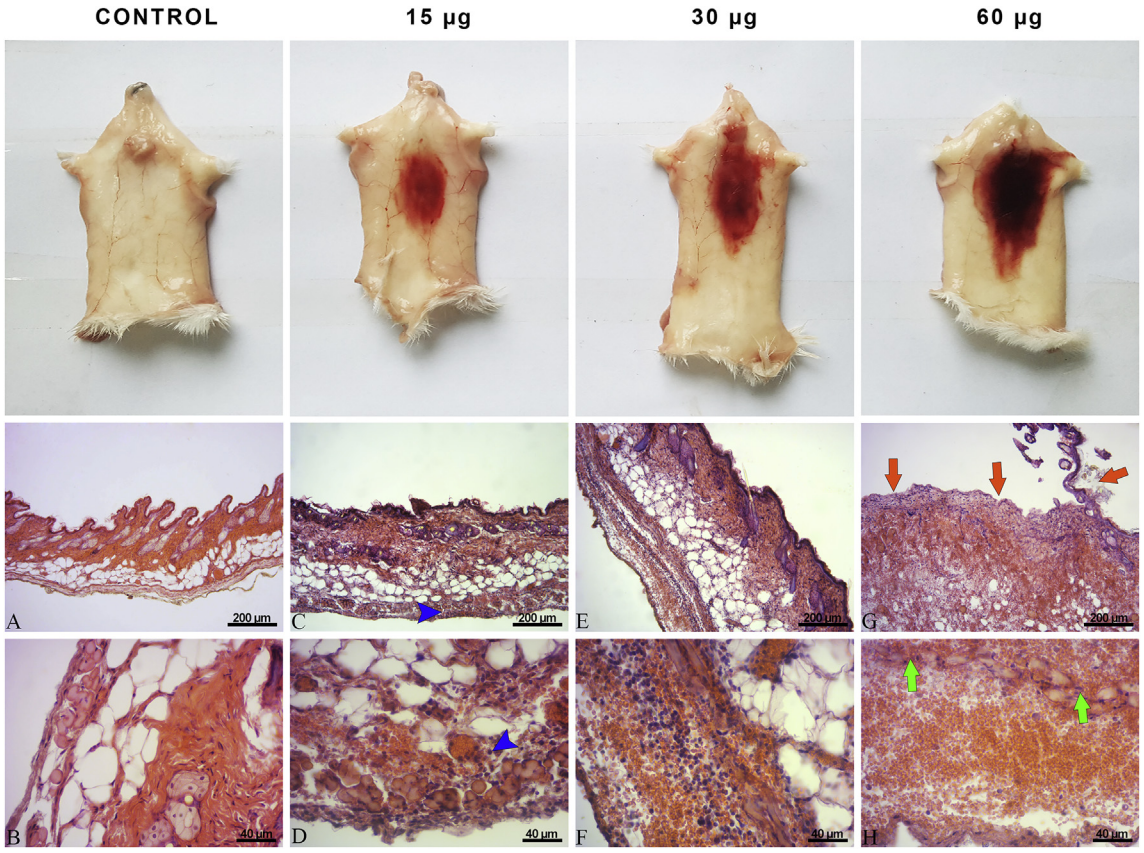

Fig. 10. Hemorrhagic assays showing gross subdermal appearance (top row) and light micrographs showing histopathological changes 2 h after injection of different amounts of *E. aesculapii* venom (µg/animal) into mouse skin (H&E stain). **A** and **B**: Control skin. **C** and **D**: Note the subcutaneous hemorrhage with leukocyte infiltration (blue arrowheads). **E** and **F**: Greater intensity of hemorrhage and inflammatory infiltrate are observed. **G** and **H**: In addition to intense hemorrhage and leukocyte infiltration, extensive detachment of epidermis and hair follicles (orange arrows) and slight myonecrosis (green arrows) are observed. (For interpretation of the references to color in this figure legend, the reader is referred to the Web version of this article.)

venom.

Snake venom is a complex secretion produced in a specialized gland that is typically delivered via a specialized envenomation system, including a secretory gland, often (but not always) specialized teeth, and a suite of specific behaviors allowing delivery of the venom (Mackessy, 2010). In the case of the species analyzed here, the venom delivery system is formed by the Duvernoy's venom glands, which exhibit histological organization similar to that described from other colubrids such as *Philodryas olfersii, Alsophis portoricensis, Leptophis ahaetulla marginatus, Clelia plumbea* and *Boiga irregularis* (de Oliveira Serapicos and Merusse, 2006; Renner and de Sabóia-Morais, 2000; Sanchez et al., 2018; Taub, 1967; Weldon and Mackessy, 2010; Zalisko and Kardong, 1992), and single rear maxillary fangs possessing a deep groove running along the rostral edge. The most striking feature of the fangs is their double-curved shape, exhibiting near their tips a beveled, blade-like appearance. The latter is a feature previously described for the ungrooved rear fangs of *Helicops modestus* (Oliveira et al., 2016), a species with piscivorous habits, and both *Hydrodynastes gigas*, a generalist feeder, and *Hypsiglena torquata*, a lizard specialist (Mackessy, 2010). However, *E. aesculapii* is an ophiophagous snake (primarily consuming terrestrial colubrid snakes) that, unlike most snake-eating species, usually swallows its prey tail first. It was suggested that scale overlap of the prey's body plays an important role in this ingestion habit (Braz and Marques, 2016).

Braz and Marques (2016) also suggested that *E. aesculapii* venom is not sufficiently potent to kill its prey, and for this reason, tail-first ingestion may have been selected as the easiest and fastest way to consume an elongated live prey item. Herein, we showed that *E. aesculapii* venom is 10 times less toxic toward mice than the venom of the coral snake *Micrurus pyrrhocryptus* (Dokmetjian et al., 2009), which is an ophiophagous snake ingesting prey head first (Greene, 1976). Although we revealed limited antigenic similarity between *E. aesculapii* venom and the most important viperid and elapid venoms from Argentina, we found that *E. aesculapii* (which resembles elapid snakes of the genus *Micrurus* in color pattern) produces a venom reminiscent of viperid venoms, containing mainly tissue-damaging toxins such as proteinases. In fact, in this work, activity of both serine and metalloproteinases were identified, similarly to viperid venoms. McGivern et al. (2014) suggested that these types of toxins could be critical for the rapid and efficient digestion of large prey items consumed by the ambush predators, such as most viperids and some colubrid snakes. In addition, based on our observations in the present study, venom yields from the specimen used herein averaged 200 µL, which is higher than that for species with active foraging ecologies and containing mainly neurotoxic components, such as *Leptophis ahaetulla marginatus* (Sanchez et al., 2018) and *Boiga irregularis* (Mackessy et al., 2006) (without treatment with ketamine/pilocarpine to stimulate yields). In the case of *E. aesculapii*, ingestion usually begins, and is completed, while the prey is still alive and moving (Braz and Marques, 2016), and the inoculation of its venom (exhibiting high hemorrhagic potency) into prey tissues may contribute to the weakness of prey that facilitates successful feeding.

Among species of *Erythrolamprus*, only the venom of *E. bizona* from Venezuela and Colombia was previously partially characterized (Lemoine and Rodríguez-Acosta, 2003; Torres-Bonilla et al., 2017). Lemoine and Rodríguez-Acosta (2003) noticed several neurotoxic symptoms in mice intraperitoneally injected with *E. bizona* venom; however, only apathy and lethargy (probably related to pain) were observed in the current study during the lethality experiments with *E.*

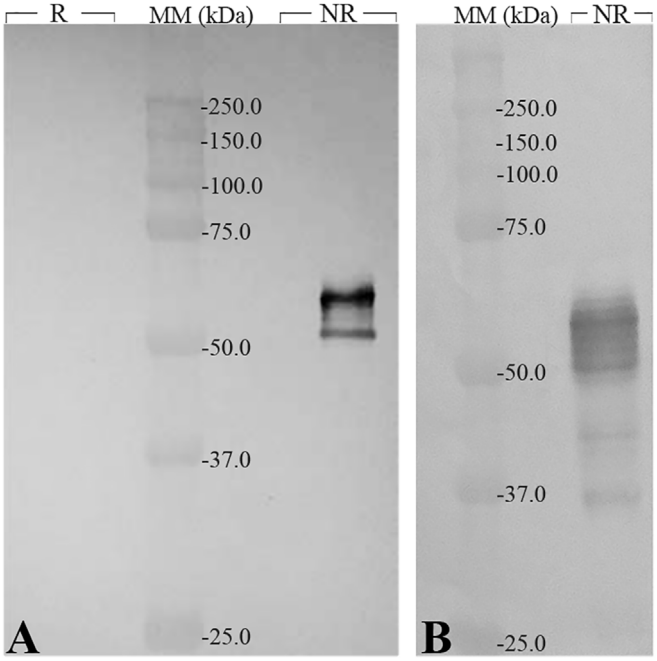

Fig. 11. Western blot analysis of venom from *E. aesculapii* using tetravalent anti-*Bothrops* (**A**) and anti-*Micrurus* (**B**) sera. Proteins were electrophoresed on a 12% SDS-PAGE gel (non-reducing conditions) and blotted onto a nitrocellulose membrane, processed as described in Materials and Methods. Note that few proteins of *E. aesculapii* venom were recognized by either antivenoms. In **A**, recognized proteins ranged from 50 to 60 kDa, whereas in **B**, proteins were recognized within the range of 37–60 kDa. MM: molecular mass markers.

aesculapii venom, without any sign/symptom of neurological alteration. In addition, although Lemoine and Rodríguez-Acosta (2003) suggested that a neurotoxic phospholipase A_2 may be responsible for the flaccid paralysis induced by the venom of *E. bizona*, we identified only a phospholipase B in *E. aesculapii* venom, and PLA_2 enzyme assays were negative. A phospholipase B exhibiting a similar molecular mass (18.5 kDa) was previously isolated from the venom of *Pseudechis colletti* (Bernheimer et al., 1987). This type of phospholipase enzyme is frequently found in relatively small amounts in several animal venoms, including snakes (e.g., Coronado et al., 2018; Modahl et al., 2018a), but its biological activity and mechanism of action in venom are poorly known.

Investigating the neuromuscular effects of *E. bizona* venom in chick biventer cervicis nerve-muscle preparations, Torres-Bonilla et al. (2017) indicated that the neuromuscular blockage resulted mainly from myotoxicity and not from neurotoxicity. These authors further suggested that muscle damage induced by this venom can be ascribed to its high proteolytic activity. In accordance, we found that the most striking biochemical feature of the venom of *E. aesculapii* is its high proteolytic activity on azocasein and azocollagen, and the level of the latter was three times higher than that exhibited by the venom of the Argentinian rear-fanged snake *Philodryas baroni* (Sánchez et al., 2014). Azocollagenolytic activity, together with its capability to degrade fibrin(ogen), suggest that *E. aesculapii* venom induces degradation of extracellular matrix components and interferes with the normal blood clot cascade, perhaps by hydrolyzing fibrinogen and disrupting the balance between fibrin formation and fibrin degradation, and both actions may be responsible for the extensive local bleeding observed in skin and gastrocnemius muscle of mice in this study. The MHD for this venom was comparable to other colubrid venoms (Sánchez et al., 2014), but it was around fourteen times higher than that of *Bothrops jararaca* venom (Antunes et al., 2010), indicating that *E. aesculapii* venom shows lower hemorrhagic activity than that of *Bothrops* venoms.

Systemic hemorrhage was particularly pronounced in animals that received lethal doses, suggesting that hypovolemic shock may be involved in fatalities. This is consistent with the findings in experimental envenomation by other rear-fanged snake venoms (Lemoine et al., 2004; Lemoine and Rodríguez-Acosta, 2003; Peichoto et al., 2006; Weldon and Mackessy, 2010). It is important to note that hyaluronidase (s) present(s) in the venom of *E. aesculapii* may contribute to the systemic distribution/diffusion of its venom toxins, though at a slower rate than that of *Bothrops* venoms (Antunes et al., 2010). Taking into account that there are very few reports of envenomation by *E. aesculapii*, and in most cases they are not well documented (Weinstein et al., 2011), these results have implications for symptoms that might be anticipated from bites by this species.

In conclusion, this work shows for the first time the biological characterization of the venom from *E. aesculapii*, as well as the main features of its venom-delivery system. Taking into account that previous works have shown that venoms from multiple individuals of rear-fanged species show conserved banding patterns and enzymatic activities (Modahl et al., 2018a; Sánchez et al., 2014), we believe that the results obtained in the current study using venom samples from only one individual of *E. aesculapii* are representative of this species. Thus, this study reveals the potential toxicological hazard of this species, which is found in forest areas frequented by humans, such as the Iguazu National Park of Argentina. It is advisable to consider this species hazardous to humans, and any medically significant accident needs to be promptly reviewed by a qualified health professional, who should be able to recognize the envenomation and provide the correct treatment to victims (alleviation of local symptoms and observation for potential coagulopathy development). There are currently 50 described species in the genus *Erythrolamprus* (http://www.reptile-database.org/), most of which may be venomous, and data presented in this paper provides insight into future directions for research on the venom of this speciose group of rear-fanged snakes.

Conflict of interest

The authors have no conflicts of interest with this work.

Acknowledgments

M.N. Sánchez is the recipient of a fellowship from Consejo Nacional de Investigaciones Científicas y Técnicas, Argentina. This work was carried out in partial fulfillment of the requirements for the PhD degree for M.N. Sánchez at the University of Buenos Aires, Argentina. We thank the National Parks Administration (APN, Argentina) for permission to collect snakes in the Iguazu National Park, and the School of Medicine of the University of Northeastern Argentina (UNNE) for providing experimental animals. We thank Agustina Quintana for technical assistance, Bertha Valdovinos Zaputovich for assistance with Alcian Blue histology, and Cecilia Galíndez and Cristina Salgado for helping with the SEM sample preparation. We are indebted to Ariel López for his assistance with snakes at the INMeT Serpentarium.

Transparency document

Transparency document related to this article can be found online at https://doi.org/10.1016/j.toxicon.2019.04.007

Funding

This work was supported by INMeT, CONICET (PIP 112-201301-00126-CO), and Agencia Nacional de Promoción Científica y Tecnológica (PICT-2013-1238) from Argentina, as well as an RDFD travel/research grant from UNC to SPM.

References

Antunes, T.C., Yamashita, K.M., Barbaro, K.C., Saiki, M., Santoro, M.L., 2010. Comparative analysis of newborn and adult *Bothrops jararaca* snake venoms. Toxicon 56, 1443–1458. https://doi.org/10.1016/j.toxicon.2010.08.011.

Arzamendia, V., Giraudo, A.R., 2012. *Erythrolamprus aesculapii* (Wied, 1821). Falsa coral misionera. Cuad. Herpetol. 26, 352.

Bernheimer, A.W., Linder, R., Weinstein, S.A., Kim, K.S., 1987. Isolation and characterization of a phospholipase B from venom of Collett's snake, *Pseudechis colletti*. Toxicon 25, 547–554.

Blum, H., Beier, H., Gross, H.J., 1987. Improved silver staining of plant proteins, RNA and DNA in polyacrylamide gels. Electrophoresis 8, 93–99. https://doi.org/10.1002/elps.1150080203.

Braz, H.B., Marques, O.A.V., 2016. Tail-first ingestion of prey by the false coral snake, *Erythrolamprus aesculapii*: does it know where the tail is? Salamandra - Ger. J. Herpetol. 52, 211–214.

Coronado, M.A., da Silva Olivier, D., Eberle, R.J., do Amaral, M.S., Arni, R.K., 2018. Modeling and molecular dynamics indicate that snake venom phospholipase B-like enzymes are Ntn-hydrolases. Toxicon 153, 106–113. https://doi.org/10.1016/j.toxicon.2018.08.014.

de Oliveira Serapicos, E., Merusse, J.L.B., 2006. Morfologia e histoquímica das glândulas de Duvernoy e supralabial de seis espécies de colubrídeos opistoglifodontes (Serpentes, Colubridae). Papéis Avulsos Zool. (São Paulo) 46, 187–195.

Dokmetjian, J.C., Del Canto, S., Vinzon, S., de Jimenez Bonino, M.B., 2009. Biochemical characterization of the *Micrurus pyrrhocryptus* venom. Toxicon 53, 375–382. https://doi.org/10.1016/j.toxicon.2008.12.015.

Ellman, G.L., Courtney, K.D., Andres Jr., V., Feather-Stone, R.M., 1961. A new and rapid colorimetric determination of acetylcholinesterase activity. Biochem. Pharmacol. 7, 88–95.

Giraudo, A.R., 2014. Diversidad e historia natural de serpientes de interés sanitario del Nordeste Argentino. In: Peichoto, M.E., Salomon, O.D. (Eds.), La problemática del ofidismo en la región Nordeste de Argentina. Una mirada científica integradora, 1ra ed. Instituto Nacional de Medicina Tropical - Ministerio de Salud de la Nación - Presidencia de la Nación, Puero Iguazú, Misiones, Argentina, pp. 10–69.

Goncalves, L.R., Mariano, M., 2000. Local haemorrhage induced by *Bothrops jararaca* venom: relationship to neurogenic inflammation. Mediat. Inflamm. 9, 101–107. https://doi.org/10.1080/096293500411569.

Greene, H.W., 1976. Scale overlap, a directional sign stimulus for prey ingestion by ophiophagous snakes. Z. Tierpsychol. 41, 113–120. https://doi.org/0.1111/j.1439-0310.1976.tb00473.x.

Junqueira-de-Azevedo, I.L., Campos, P.F., Ching, A.T., Mackessy, S.P., 2016. Colubrid venom composition: an -omics perspective. Toxins 8, 230. https://doi.org/10.3390/toxins8080230.

Laemmli, U.K., 1970. Cleavage of structural proteins during the assembly of the head of bacteriophage T4. Nature 227, 680–685.

Lema, T., 1978. Cobras não venenosas que matam. Nat. Rev. 4, 38–46.

Lemoine, K., Giron, M.E., Aguilar, I., Navarrete, L.F., Rodriguez-Acosta, A., 2004. Proteolytic, hemorrhagic, and neurotoxic activities caused by *Leptodeira annulata ashmeadii* (Serpentes: colubridae) Duvernoy's gland secretion. Wilderness Environ. Med. 15, 82–89.

Lemoine, K., Rodríguez-Acosta, A., 2003. Hemorrhagic, proteolytic and neurotoxic activities produced by Duvernoy's gland secretion from the false coral snake (*Erythrolamprus bizona* Jan 1863)(Serpentes: colubridae). Revista Científica FCV-LUZ 13, 371–377.

Mackessy, S.P., 2010. In: Mackessy, S.P. (Ed.), Handbook of Venoms and Toxins of Reptiles, 1 ed. CRC Press - Taylor and Francis Group, Boca Raton, pp. 528.

Mackessy, S.P., Sixberry, N.M., Heyborne, W.H., Fritts, T., 2006. Venom of the Brown Treesnake, *Boiga irregularis*: ontogenetic shifts and taxa-specific toxicity. Toxicon 47, 537–548. https://doi.org/10.1016/j.toxicon.2006.01.007.

McGivern, J.J., Wray, K.P., Margres, M.J., Couch, M.E., Mackessy, S.P., Rokyta, D.R., 2014. RNA-seq and high-definition mass spectrometry reveal the complex and divergent venoms of two rear-fanged colubrid snakes. BMC Genomics 15, 1061. https://doi.org/10.1186/1471-2164-15-1061.

Minton, S.A., 1990. Venomous bites by nonvenomous snakes: an annotated bibliography of colubrid envenomation. J. Wilderness Med. 1, 119–127.

Modahl, C.M., Frietze, S., Mackessy, S.P., 2018a. Transcriptome-facilitated proteomic characterization of rear-fanged snake venoms reveal abundant metalloproteinases with enhanced activity. J. Proteom. 187, 223–234. https://doi.org/10.1016/j.jprot.2018.08.004.

Modahl, C.M., Mrinalini, Frietze, S., Mackessy, S.P., 2018b. Adaptive evolution of distinct prey-specific toxin genes in rear-fanged snake venom. Proc. Biol. Sci. 285. https://doi.org/10.1098/rspb.2018.1003.

National Research Council, 1996. Guide for the Care and Use of Laboratory Animals. The National Academies Press, Washington, DC, pp. 140.

Oliveira, L., Scartozzoni, R.R., Almeida-Santos, S.M., Jared, C., Antoniazzi, M.M., Salomão, M.G., 2016. Morphology of Duvernoy's glands and maxillary teeth and a possible function of the Duvernoy's gland secretion in *Helicops modestus* Günther, 1861 (Serpentes: xenodontinae). South Am. J. Herpetol. 11, 54–65. https://doi.org/10.2994/sajh-d-16-00011.1.

Peichoto, M.E., Teibler, P., Ruiz, R., Leiva, L., Acosta, O., 2006. Systemic pathological alterations caused by *Philodryas patagoniensis* colubrid snake venom in rats. Toxicon 48, 520–528. https://doi.org/10.1016/j.toxicon.2006.06.013.

Pla, D., Petras, D., Saviola, A.J., Modahl, C.M., Sanz, L., Perez, A., Juarez, E., Frietze, S., Dorrestein, P.C., Mackessy, S.P., Calvete, J.J., 2018. Transcriptomics-guided bottom-up and top-down venomics of neonate and adult specimens of the arboreal rear-fanged Brown Treesnake, *Boiga irregularis*, from Guam. J. Proteom. 174, 71–84. https://doi.org/10.1016/j.jprot.2017.12.020.

Quelch, J.J., 1893. Venom in harmless snakes. Zool. J. Linn. Soc. 17 31-31.

Quintana, M.A., Sciani, J.M., Auada, A.V.V., Martinez, M.M., Sanchez, M.N., Santoro, M.L., Fan, H.W., Peichoto, M.E., 2017. Stinging caterpillars from the genera *Podalia, Leucanella* and *Lonomia* in Misiones, Argentina: a preliminary comparative approach to understand their toxicity. Comparative Biochemistry and Physiology part C. Toxicol. Pharmacol. 202, 55–62. https://doi.org/10.1016/j.cbpc.2017.07.007.

Renner, M.F., de Sabóia-Morais, S.M.T., 2000. Estudo histológico e histoquímico da glândula de Duvernoy de *Clelia plumbea* (Wied) (Serpentes, Colubridae, Xenodontinae). Rev. Bras. Zool. 17, 583–588.

Sanchez, M.N., Teibler, G.P., Lopez, C.A., Mackessy, S.P., Peichoto, M.E., 2018. Assessment of the potential toxicological hazard of the Green Parrot Snake (*Leptophis ahaetulla marginatus*): characterization of its venom and venom-delivery system. Toxicon 148, 202–212. https://doi.org/10.1016/j.toxicon.2018.04.027.

Sánchez, M.N., Timoniuk, A., Maruñak, S., Teibler, P., Acosta, O., Peichoto, M.E., 2014. Biochemical and biological analysis of *Philodryas baroni* (Baron's Green Racer; Dipsadidae) venom Relevance to the findings of human risk assessment. Hum. Exp. Toxicol. 33, 22–31. https://doi.org/10.1177/0960327113493302.

Saviola, A.J., Peichoto, M.E., Mackessy, S.P., 2014. Rear-fanged snake venoms: an untapped source of novel compounds and potential drug leads. Toxin Rev. 33, 185–201. https://doi.org/10.3109/15569543.2014.942040.

Schägger, H., von Jagow, G., 1987. Tricine-sodium dodecyl sulfate-polyacrylamide gel electrophoresis for the separation of proteins in the range from 1 to 100 kDa. Anal. Biochem. 166, 368–379.

Taub, A.M., 1967. Comparative histological studies on Duvernoy's gland of colubrid snakes. Bull. Am. Mus. Nat. Hist. 138, 1–50 New York.

Torres-Bonilla, K.A., Floriano, R.S., Schezaro-Ramos, R., Rodrigues-Simioni, L., da Cruz-Hofling, M.A., 2017. A survey on some biochemical and pharmacological activities of venom from two Colombian colubrid snakes, *Erythrolamprus bizona* (Double-banded coral snake mimic) and *Pseudoboa neuwiedii* (Neuwied's false boa). Toxicon 131, 29–36. https://doi.org/10.1016/j.toxicon.2017.02.030.

Weinstein, S.A., Warrell, D.A., White, J., Keyler, D.E., 2011. Venomous" Bites from Non-venomous Snakes: a Critical Analysis of Risk and Management of “Colubrid" Snake Bites. Elsevier, London, pp. 336.

Weldon, C.L., Mackessy, S.P., 2010. Biological and proteomic analysis of venom from the Puerto Rican Racer (*Alsophis portoricensis*: dipsadidae). Toxicon 55, 558–569. https://doi.org/10.1016/j.toxicon.2009.10.010.

Zalisko, E.J., Kardong, K.V., 1992. Histology and Histochemistry of the Duvernoy's Gland of the Brown Tree Snake Boiga Irregularis (Colubridae). pp. 791–799 Copeia.